N62 60539

NACA RM L50G19a

TECH LIBRARY KAFB, NM
0143811

RESEARCH MEMORANDUM

7205

PRELIMINARY INVESTIGATION OF REFLECTIONS OF OBLIQUE WAVES FROM A POROUS WALL

By Don D. Davis, Jr., and George P. Wood

Langley Aeronautical Laboratory
Langley Air Force Base, Va.

AFOSR Technical Library
Apr 2291

NATIONAL ADVISORY COMMITTEE
FOR AERONAUTICS
WASHINGTON

November 9, 1950
Declassified March 10, 1954

TECH LIBRARY KAFB, NM
0143811

NATIONAL ADVISORY COMMITTEE FOR AERONAUTICS

RESEARCH MEMORANDUM

PRELIMINARY INVESTIGATION OF REFLECTIONS OF OBLIQUE WAVES FROM A POROUS WALL

By Don D. Davis, Jr., and George P. Wood

SUMMARY

A porous wall was used in an attempt to eliminate reflections of oblique waves from a tunnel wall. Calculations were made of the required resistance characteristics of a wall in order that the flow through the wall, due to the pressure difference across a shock wave, would equal the component normal to the wall of the flow behind the shock wave. The resistance characteristic of a sintered bronze wall was measured and the reflections of waves impinging on the wall were observed at a Mach number of 1.62. The intensity of the reflections was greatly reduced by permitting flow through the wall.

INTRODUCTION

Two of the well-known difficulties encountered in wind-tunnel testing at transonic speeds are: first, the necessity of changing nozzles in order to change the test-section Mach number from high-subsonic to low-supersonic speeds and of using a different nozzle for each different supersonic Mach number, and second, the necessity of using a model that is small enough, compared to the size of the test section, so that wall-interference effects are negligibly small. In an effort to alleviate these difficulties, the slotted-wall tunnel has been proposed. As presently developed, the slotted-wall tunnel has been shown to give results that are in fair agreement through the transonic range up to a Mach number of 1.08 with the free-air flow around a nonlifting body that is relatively large compared to the size of the body that can be tested in a tunnel with solid walls (ref. 1). At Mach numbers higher than 1.08, there are local disturbances in the pressure distribution on the model that are believed to be due to reflections of the model bow wave from the slotted wall.

One of the well-known difficulties in testing at supersonic speeds is that caused by reflections of shock waves from the tunnel walls.

The model must be small enough so that reflections of upstream flow disturbances from the model do not impinge on it. The present paper reports the results of an attempt to find a means of alleviating the limitations on model size in testing at supersonic speeds by using a porous wall to eliminate, or to weaken considerably, reflections from the wall. The leading edge of a wedge, for example, the lower surface of which is at a positive angle of attack with respect to the free stream, produces a shock wave (fig. 1). Behind the shock wave the pressure is higher than free-stream pressure and the flow direction is parallel to the surface of the wedge, and, therefore, has a component normal to the wall of the test section. If the wall is solid, the shock-wave incident on it is reflected as a shock wave that turns the flow back to a direction parallel with the wall. The boundary condition of no flow into a solid wall is thus satisfied. In an open-throat tunnel, on the other hand, a shock-wave incident on the free boundary is reflected as an expansion, as there must be no pressure difference across the boundary.

Qualitatively, then, the solid wall furnishes too much restraint, producing a reflected shock wave, while the open throat furnishes too little restraint, producing a reflected expansion wave. For the present tests it was believed that if a restraint between that provided by the open throat and that provided by the solid wall were used, the reflection might be eliminated. A porous wall offers a partial restraint that is, in general, more evenly distributed than that of a slotted wall. It was believed that by using a wall of the correct porosity, the rise in pressure across the incident shock wave might be used to induce a flow through the porous wall of a magnitude equal to the normal component of the flow behind the incident shock wave. Under that condition it might be expected that there would be no reflection from the wall to propagate back into the stream and impinge on the model.

An analysis was made to determine the order of magnitude of the porosity required for various angles of deviation at free-stream Mach numbers of 1.30 and 1.62. Observations were then made of the reflections from a porous wall with a free-stream Mach number of 1.62. The tests were made in March 1949 and are the "prior experimentation" mentioned in reference 2, which presents the results of another investigation of shock reflection from porous walls. A much lower Mach number, 1.18, was used for the tests reported in reference 2 than was used for the tests reported herein.

SYMBOLS

a	velocity of sound
M	Mach number

p	static pressure
R	gas constant
S	fringe shift
T	temperature
V	velocity
V_n	component of velocity normal to wall (see fig. 1)
γ	ratio of specific heats (1.4 for air)
δ	angle of deviation of flow across shock wave (see fig. 1)
ϵ	angle of shock wave (see fig. 1)
ρ	density

Subscripts:

0	stagnation conditions ahead of shock wave
1	free stream
2	behind shock wave

ANALYSIS

The pressure p_2 behind an oblique shock wave (fig. 1) is greater than the pressure p_1 ahead of the shock wave. The pressure difference across the shock wave is given by the equation

$$\frac{p_2 - p_1}{p_1} = \frac{2\gamma}{\gamma + 1}\left(M_1^2 \sin^2\epsilon - 1\right) \tag{1}$$

The assumptions are made that the free-stream pressure p_1 ahead of the shock wave is atmospheric pressure and that the pressure outside of the porous wall on which the shock wave is incident is also atmospheric pressure. Therefore, the pressure difference across the shock wave is also the pressure difference across the porous wall if there is no reflection from the wall. (See fig. 1.) The assumptions are now made

that there will be no reflection from the wall if air flows through the wall at the correct rate, and that the correct rate of flow is $\rho_2 V_n$. The quantities ρ_2 and V_n are given, respectively, by the equations

$$\frac{\rho_2}{\rho_1} = \frac{\tan \epsilon}{\tan(\epsilon - \delta)} \tag{2}$$

$$\frac{V_n}{V_1} = \frac{\cos \epsilon \sin \delta}{\cos(\epsilon - \delta)} \tag{3}$$

The shock-wave angle ϵ and the flow deviation δ are related by the equation

$$\frac{\cot \delta}{\tan \epsilon} + 1 = \frac{\frac{\gamma + 1}{2} M_1^2}{M_1^2 \sin^2 \epsilon - 1} \tag{4}$$

Equations (1) to (4) can be used to find the relation between the pressure difference $p_2 - p_1$ available across a porous wall and the required rate of flow $\rho_2 V_n$ through the wall for a given free-stream Mach number and various values of the flow deviation δ. The values for pressure difference and the rate of flow were converted to the non-dimensional ratios $\frac{p_2 - p_1}{p_o}$ and $\frac{\rho_2 V_n}{\rho_o a_o}$, respectively, by the use of the stagnation conditions ahead of the shock wave, which conditions are given by the equations:

$$p_o = p_1 \left(1 + \frac{\gamma - 1}{2} M_1^2\right)^{\frac{\gamma}{\gamma - 1}} \tag{5}$$

$$\rho_o = \rho_1 \left(1 + \frac{\gamma - 1}{2} M_1^2\right)^{\frac{\gamma}{\gamma - 1}} \tag{6}$$

$$T_o = T_1 \left(1 + \frac{\gamma - 1}{2} M_1^2\right) \tag{7}$$

$$a_o = (\gamma R T_o)^{1/2} \tag{8}$$

Equations (1) to (8) were used to obtain the curves in figure 2. (The tables and charts of ref. 3 were useful in making the computations.) These curves show the nondimensional pressure difference as a function of the nondimensional rate of flow normal to the wall for two free-stream Mach numbers, 1.30 and 1.62, and over a range of angles of deviation of the flow. The curves of figure 2 thus represent the desired characteristics of a porous wall.

A similar analysis is possible for a calculable three-dimensional flow, such as conical flow. The two-dimensional case is, however, very much easier to handle in both analysis and experiment.

APPARATUS

The tests were conducted in a 3-inch-square jet in which the free-stream Mach number was 1.62. The jet was open, or free, on three sides. On the fourth side, one of the side walls of the two-dimensional nozzle was extended and in this side wall a porous plate was inserted to form a porous wall. The under side of the porous wall was open to the atmosphere. Figure 3 is a schematic diagram of the nozzle and the porous wall.

In the free stream above the porous wall a double-wedge airfoil, of 5.85° included angle, was supported by a sting in such a position that a shock wave or an expansion wave from the leading edge of the wedge impinged on the porous wall. The angle of attack of the wedge could be varied. A Mach-Zehnder interferometer was used for making observations of the flow. The field of view of the interferometer is indicated in figure 3. Interferograms were taken that showed the wave incident on the porous wall and the reflection of the wave from the wall.

The porous wall used in this investigation was a plate of sintered bronze, approximately 1/16 inch thick. The plate was glued to a supporting frame of wood, as shown in figure 4, which shows the outside, or bottom, surface of the plate. This unit was then mounted in a slot in a solid steel nozzle side wall (fig. 5). Care was used to obtain a smooth juncture at the front edge. The porous section between the inner edges of the wood frame completely spanned one side of the supersonic jet. The face of the sintered bronze plate was lightly sanded to reduce the surface roughness somewhat. The plate was oriented so that the porosity appeared nearly constant across the plate at any given axial station, but there was a visually obvious porosity variation with distance in the direction of the jet axis.

The pressure-drop characteristics of the sintered-bronze plate were determined with a device which forced air through a $\frac{3}{4}$- inch-diameter

section of the bronze plate while sealing the rest of the plate to prevent lateral flow. An orifice was used in the measurement of velocity. Calibrations were made with the tester at three transverse locations at the axial station where the disturbance reached the surface in most of the experiments. The measured characteristics of the plate are shown in figure 6, in which the pressure difference across the plate is plotted against $\frac{1}{2}\rho V_n^2$. The plate was calibrated at approximately atmospheric density. Figure 6 also shows the calculated wall requirements based on the experimental flow conditions: a free-stream Mach number of 1.62, free-stream density of 0.00355 slug per cubic foot, free-stream velocity of 1480 feet per second, and stagnation temperature of 70° F.

The porous bronze wall matched the calculated requirements for a flow-deflection angle of slightly above $\frac{1}{2}^\circ$; for higher angles it was too dense. A careful search of all commercially available porous materials revealed that although this material did not match the requirements exactly, it was the most nearly suitable type available.

The interferograms that were taken of the flow pattern have the disadvantage that accurate quantitative evaluation of them was not possible because of disturbances from the free sides of the jet. In an open jet the pressure in the free stream is atmospheric pressure, and the pressure behind a shock wave is greater than atmospheric pressure. A free jet boundary, however, cannot support a pressure difference; therefore, where a shock wave impinges on a free jet boundary, an expansion wave is reflected back into the stream in order to maintain atmospheric pressure at the boundary of the jet. In fact, wherever a wave impinges on a free boundary, a wave of opposite sign is generated. In the interferograms that are discussed herein, a wave extends from the leading edge of a wedge to the porous plate and is reflected back into the flow, but where the sides of both the incident and the reflected waves intersect the free jet boundaries, in a plane that is at right angles to the porous plate, reflected waves are produced that propagate back into the flow. The presence of these waves prevents an accurate quantitative evaluation of the interferograms. For that reason, the interferograms are used only for making qualitative observations on the strength relative to each other of the waves incident on and reflected from the porous plate.

RESULTS AND DISCUSSION

Figure 7 shows the interference pattern in the test region without air flow. The extended nozzle side plate in which the porous plate is inserted is in the lower part of the figure. The forward portion of the wedge is also shown.

Figure 8 is an interferogram of the flow with the lower surface of the wedge at an angle of 5° to the axis of the supersonic jet at a Mach number of 1.62. This picture shows the reflection of a shock wave from a solid wall. The intensity of a disturbance is indicated on an interferogram by the amount, measured in number of interference fringes, by which a fringe is displaced in the disturbance. This fringe displacement is a linear function of the density change across the disturbance in accordance with the following relation:

$$\frac{\rho_2}{\rho_1} = 1 + \text{Constant} \times S$$

The constant is a function of the optical system and S is the fringe displacement. In the interferograms presented here, a downward displacement of the fringes indicates a compression and an upward shift indicates an expansion. In theory, the flow deflection across a reflection from a straight solid wall should be equal to the deflection across the original shock wave. Inspection of figure 8 indicates that the reflection is a disturbance of the same order of magnitude as the incident shock wave. The boundary layer on the solid wall is shown by the closely packed interference fringes that lie near the wall and approximately parallel to it. The vertical distance between the porous plate and the leading edge of the wedge is 1 inch. The interferogram has been magnified sufficiently so that the influence of the boundary layer on the shock wave in the region near the boundary layer is visible.

Figure 9(a) is an interferogram of the flow with the porous wall in place. The angle of the lower surface of the wedge is set at $3\frac{3}{4}^\circ$ and the Mach number is 1.62. The disturbance that lies on and above the upper surface of the wedge and that begins between the leading edge of the wedge and the sting support is due to a bow wave generated by the support. The shock wave from the leading edge of the wedge is shown impinging on the porous plate at the point where the calibration (fig. 6) was obtained. The shock wave is of such intensity that in it the fringes are displaced by approximately six fringe widths. This fact is shown by the heavy line that has been drawn along a fringe through the shock wave (The shock wave is of great enough intensity that the fringes are packed so closely in the wave that a fringe cannot be followed directly through a wave. The place where a fringe emerges from the wave can be determined, however, by counting fringes into the boundary layer, then following a fringe past the region of the incident shock, and then counting fringes up into the main flow.) The reflection from the porous wall of the incident shock wave is also shown and is seen to be an expansion followed by a compression. The net fringe shift across the reflected disturbance is, therefore, more diffuse and much less intense than the incident

disturbance, even though the calibration and calculations indicate that the porosity of the plate is considerably different from that required to cancel completely the incident shock wave. This result is in contrast with the results for the solid wall (fig. 8) in which the reflected wave appeared to be of about the same strength and character as the incident wave.

Figure 9(b) shows the flow with the lower surface of the wedge at $1\frac{3}{4}^\circ$. The fringe displacement in the incident wave is approximately three fringe widths. The reflected wave is more diffuse and of smaller intensity than the incident shock wave. In fact, the reflected disturbance has only a very small intensity near the wedge. In this case, then, the porosity of the plate was such that the reflection of the particular shock wave under discussion was nearly canceled. This indicates that concentrated disturbances probably can be eliminated.

Although the reflection is so weak that it is not clear from the interferogram whether it is a compression or an expansion, the calibration of figure 6 indicates that the material is too dense to meet the calculated requirements for exact cancellation at $\delta = 1\frac{3}{4}^\circ$. A reflected compression is therefore to be expected. Using the calibration given in figure 6, the strength of the reflected wave has been calculated for an incident shock wave with $\delta = 1\frac{3}{4}^\circ$. The results indicate that a reflection is to be expected corresponding to a deviation angle δ of about $\frac{1}{2}^\circ$. Thus, in spite of the apparent wide deviation of the porous-wall calibration from the calculated wall requirements, the weak reflection found in figure 9(b) is in qualitative agreement with the calculations. Because the jet density was higher than atmospheric it was necessary to assume in the calculations that the pressure drop across the sintered bronze was proportional to the density.

Inasmuch as the porosity of the plate varied in a longitudinal direction, the wedge was moved three-quarters of an inch toward the nozzle in order that the shock wave from the leading edge would be incident on a portion of the plate that was more porous. The angle of attack of the lower surface of the wedge remained at $1\frac{3}{4}^\circ$. The interferogram of the flow is shown in figure 9(c). In this case the reflected disturbance is an expansion wave. The fringe displacement in the incident shock wave is again approximately three fringe widths, and in the reflected expansion wave the displacement is approximately two fringe widths. The porosity of the plate at this location is too great for cancellation of the incident shock wave and is, in fact, great enough to cause the shock wave to be reflected as an expansion wave.

Figure 9(c) also shows that the boundary layer on the wall becomes thinner behind the incident shock wave. Both the incident shock wave and the reflected expansion wave turn the flow toward the wall and, in contrast to the solid-wall case, part of the air goes out through the porous wall. The boundary layer is thinned as a result of this outflow.

To observe the reflection of an expansion wave, the lower surface of the wedge was set at a negative angle of attack of $2\frac{3}{4}^\circ$. Figure 10(a) is an interferogram of the resulting flow. The difficulty of obtaining a pure expansion wave from the leading edge of a wedge is well known. As is usually the case, in the present instance the expansion wave is preceded by a shock wave. The downward displacement of the fringe occurs in the shock wave and the upward displacement in the expansion wave. The reflection of the disturbance is a compression which has less intensity than the original disturbance. Because of this fact, the pressure behind the compression is less than atmospheric pressure and a flow is induced upward through the porous wall from the ambient air into the stream. This flow is indicated in figure 10(a) by the increasing thickness of the boundary layer in the direction of flow behind the compression.

In figure 10(b) the lower surface of the wedge is at a negative angle of attack of 8°. The results are qualitatively the same as for figure 10(a).

The interferograms which have been presented show that in some cases nearly complete cancellation of the reflections was obtained. They thus tend to substantiate the premise upon which this work was based. On the basis of this exploratory investigation further experiments with more suitable porous materials with a test facility which will permit a quantitative evaluation of the reflected disturbances are desirable.

CONCLUDING REMARKS

1. The wall porosity, in the form of curves of pressure difference against flow rate, required for the elimination of reflections from the wall of oblique shock waves in two-dimensional flow has been calculated and presented for two Mach numbers. The curves are different for the two Mach numbers.

2. The experiments indicate that if the correct amount of the air behind a shock-wave incident on a porous wall is caused to flow out through the wall, the reflection of a single shock wave from the wall can probably be eliminated. The experimental results show that even in those cases where the porous wall is much too dense to eliminate the

reflections, the wall will considerably reduce the intensity of the reflections.

3. Although no calculations have been presented for the case of reflections of expansion waves, the experiments show that the intensity of these can also be reduced by a porous wall.

Langley Aeronautical Laboratory
National Advisory Committee for Aeronautics
Langley Air Force Base, Va.

REFERENCES

1. Ward, Vernon G., Whitcomb, Charles F., and Pearson, Merwin D.: An NACA Transonic Test Section with Tapered Slots Tested at Mach Numbers to 1.26. NACA RM L50B14, 1950.

2. Nelson, William J., and Bloetscher, Frederick: Preliminary Investigation of Porous Walls as a Means of Reducing Tunnel Boundary Effects at Low-Supersonic Mach Numbers. NACA RM L50D27, 1950.

3. Neice, Mary M.: Tables and Charts of Flow Parameters across Oblique Shocks. NACA TN 1673, 1948.

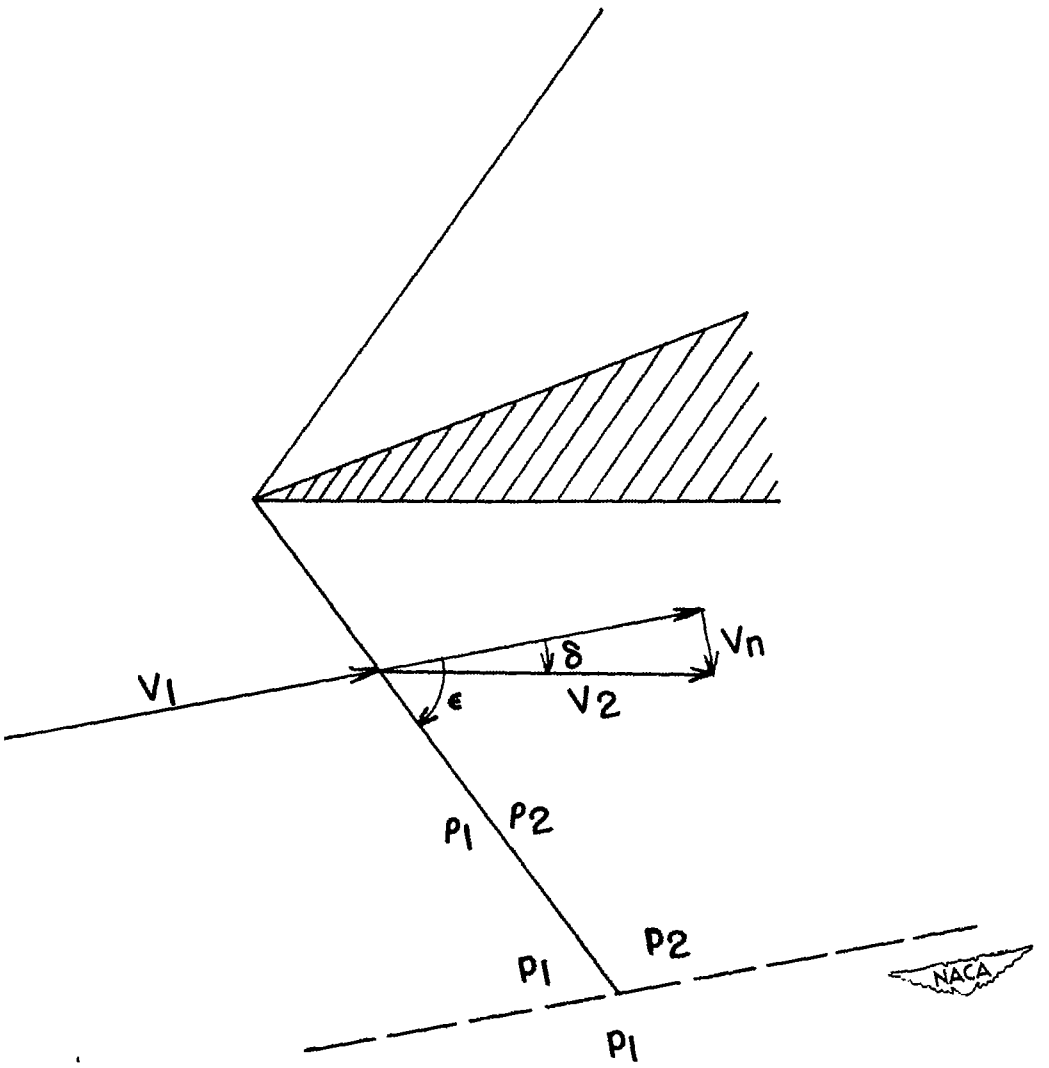

Figure 1.- Sketch showing deviation of flow by a two-dimensional oblique shock wave.

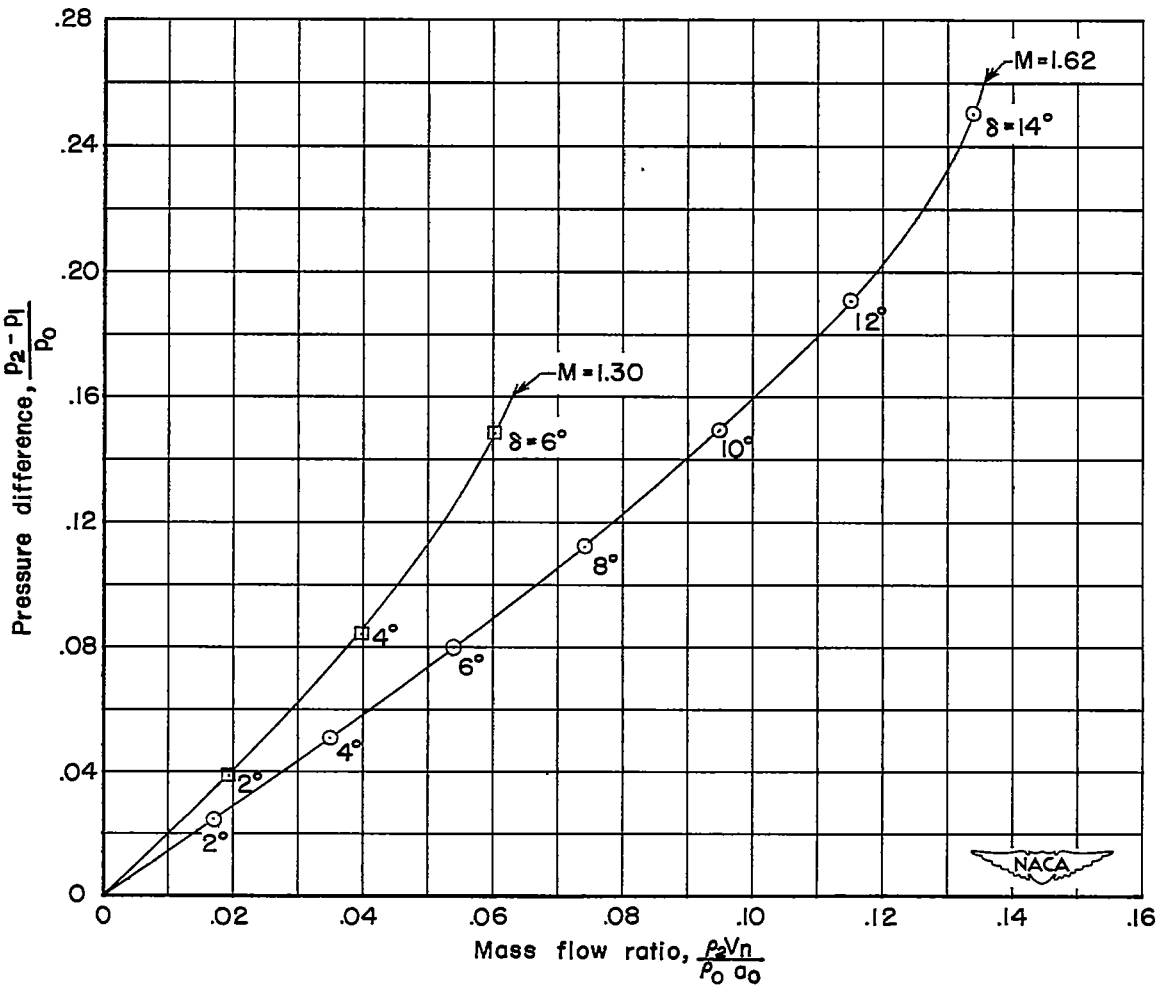

Figure 2.- Calculated conditions for elimination of shock reflection.

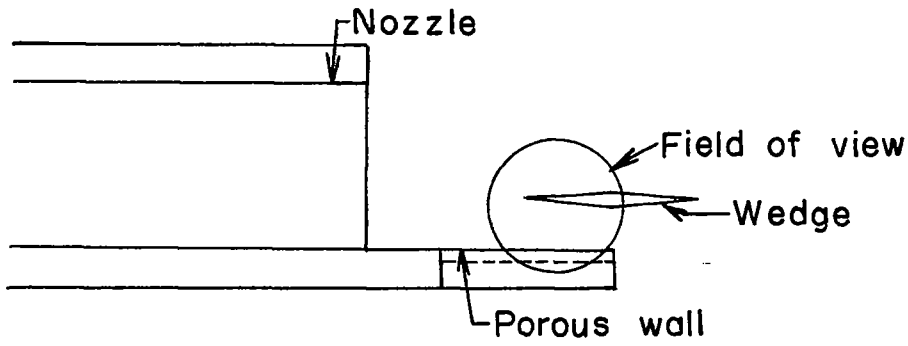

(a) Elevation.

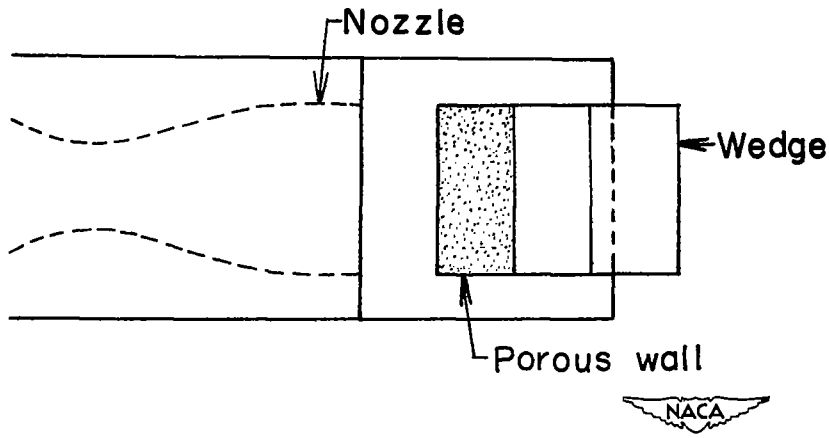

(b) Plan.

Figure 3.- Nozzle and porous wall arrangement.

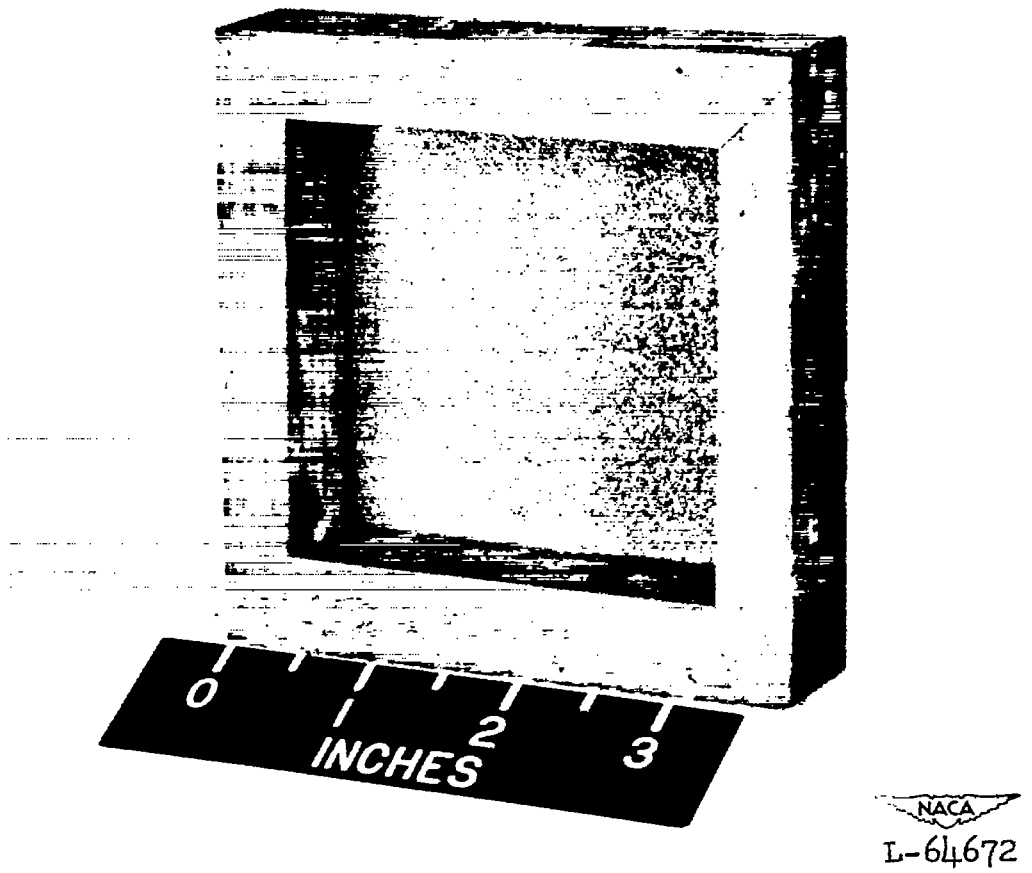

Figure 4.- Bottom view of sintered-bronze wall glued to supporting wooden frame.

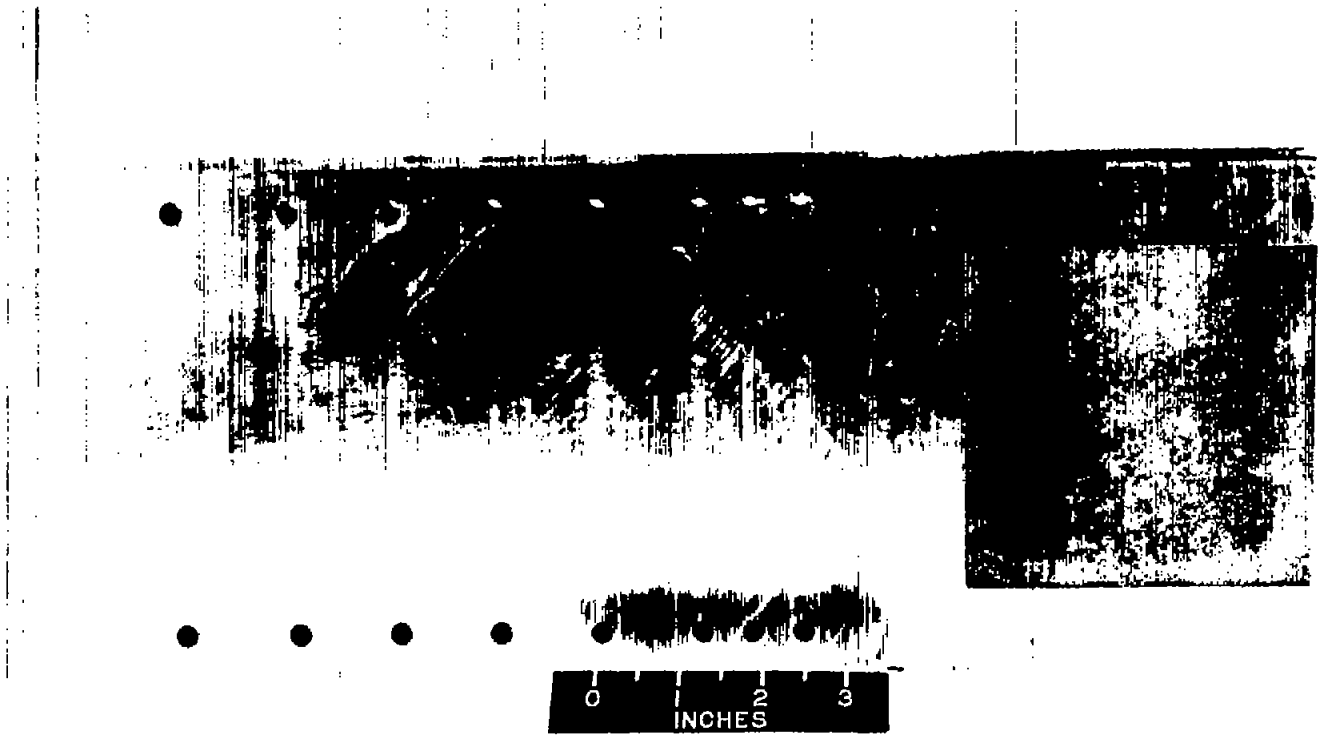

NACA
L-64671

Figure 5.- Porous wall of sintered bronze mounted in a steel nozzle block.

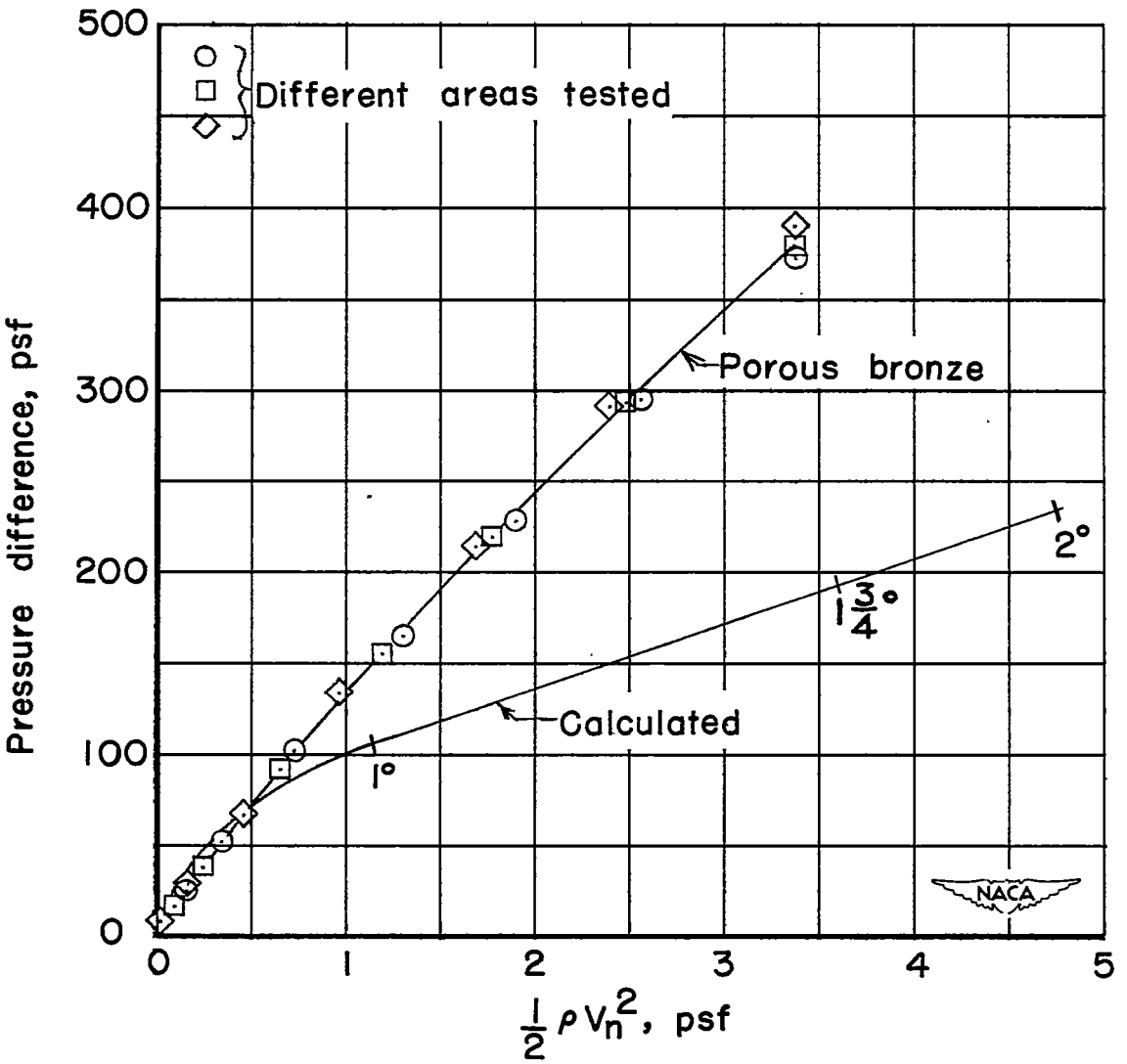

Figure 6.- Calibration of porous bronze wall compared with calculated wall requirements. Calculations for $M_1 = 1.62$, $\rho_1 = 0.00355$ slug per cubic foot, $T_0 = 70^\circ$ F.

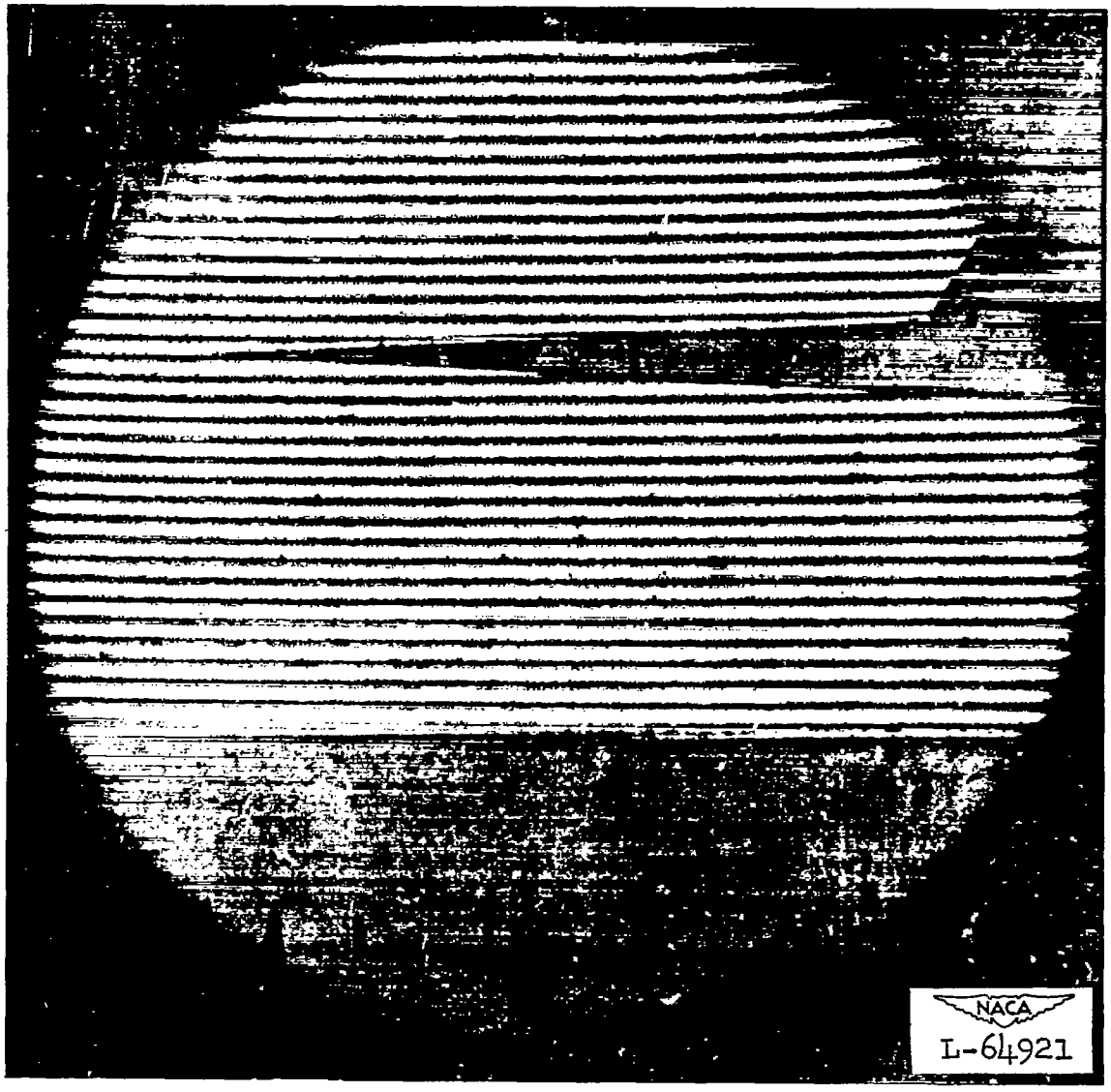

Figure 7.- Interference pattern without air flow.

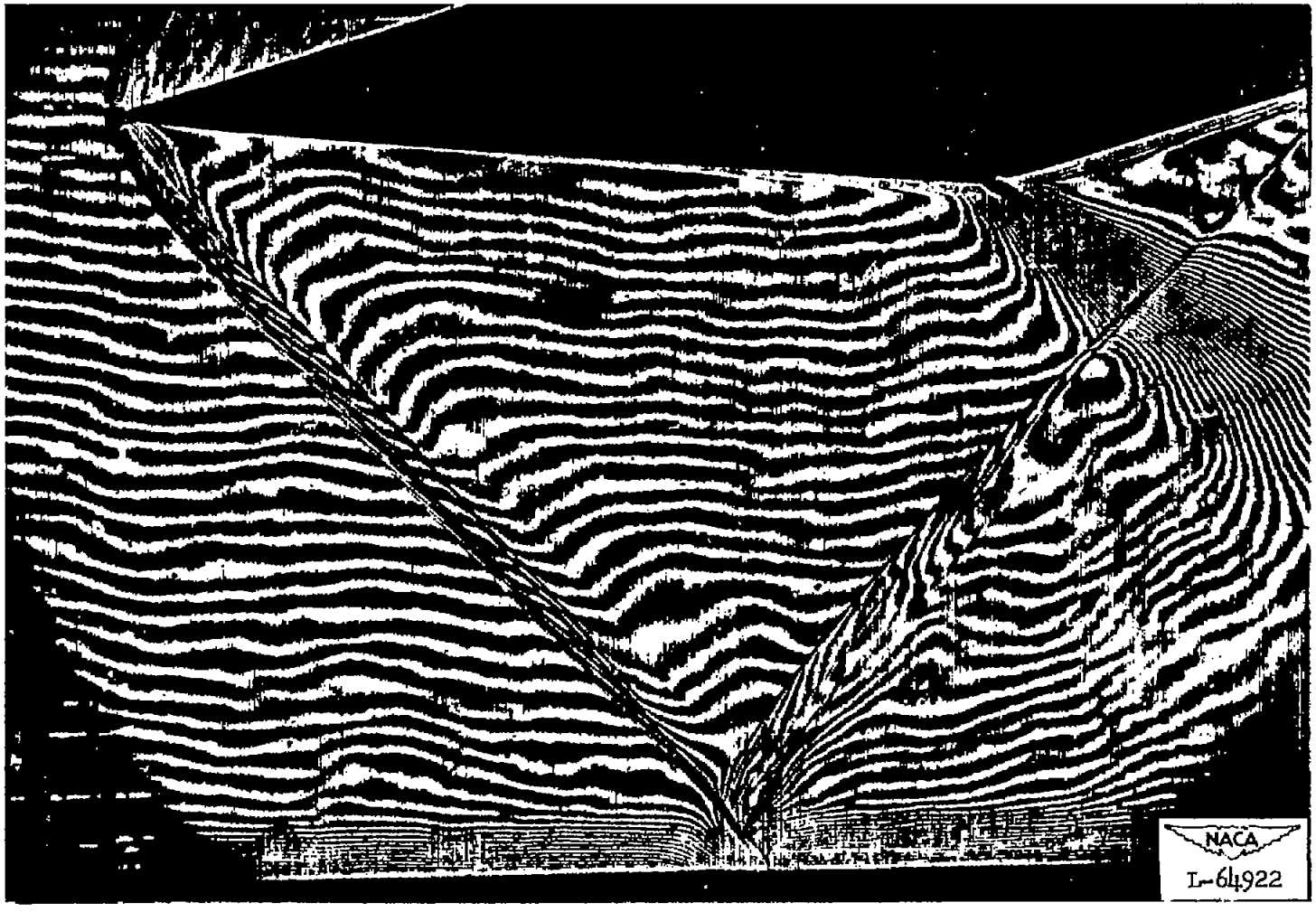

Figure 8.- Interferogram of flow in the region between a wedge and a solid wall, with a shock wave generated at the leading edge of the wedge. $\delta = 5^{\circ}$; M = 1.62.

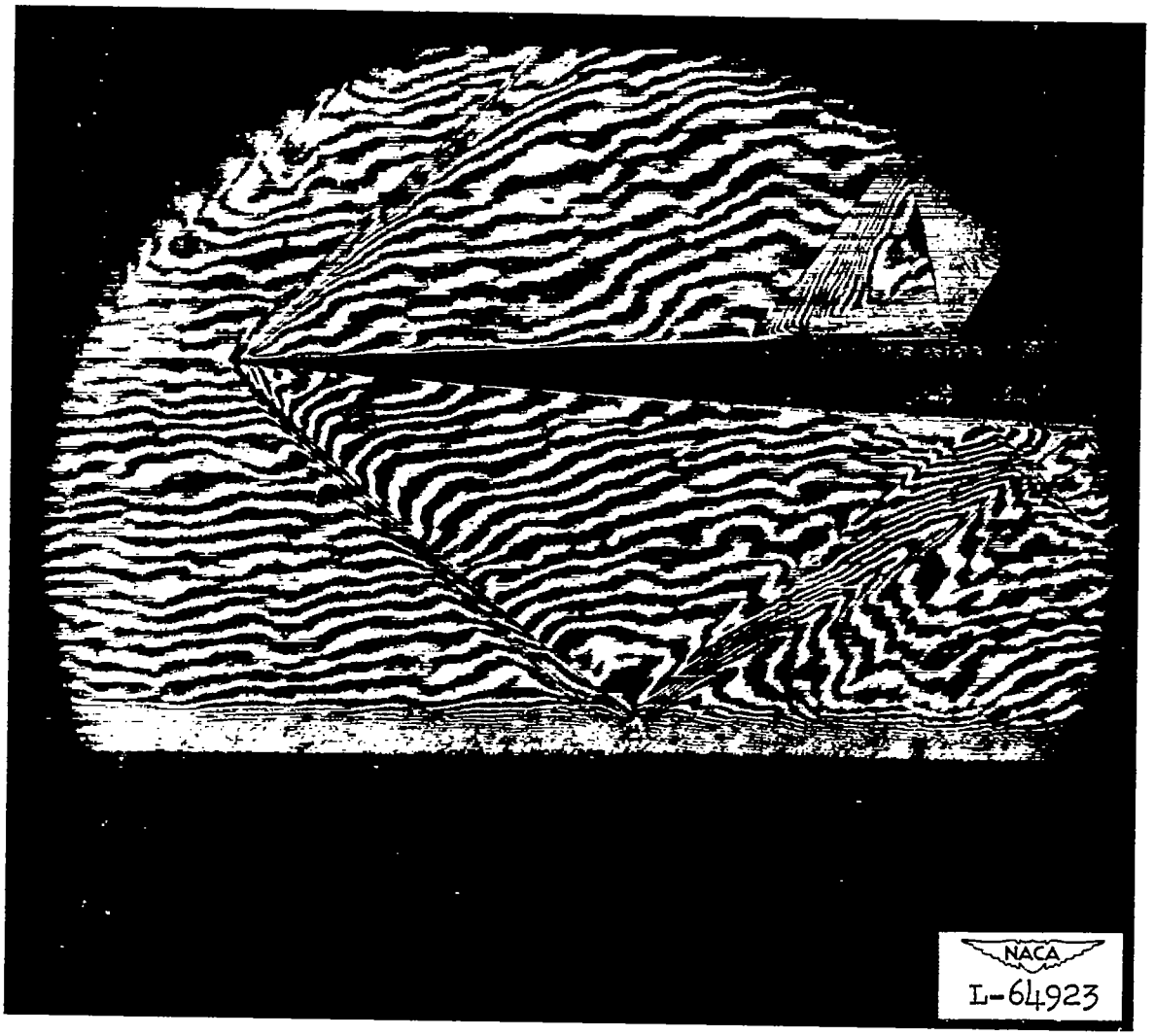

(a) $\delta = 3\frac{3}{4}^{\circ}$.

Figure 9.- Interferogram of flow in the region between a wedge and a porous wall at a Mach number of 1.62, with a shock wave generated at the leading edge of the wedge.

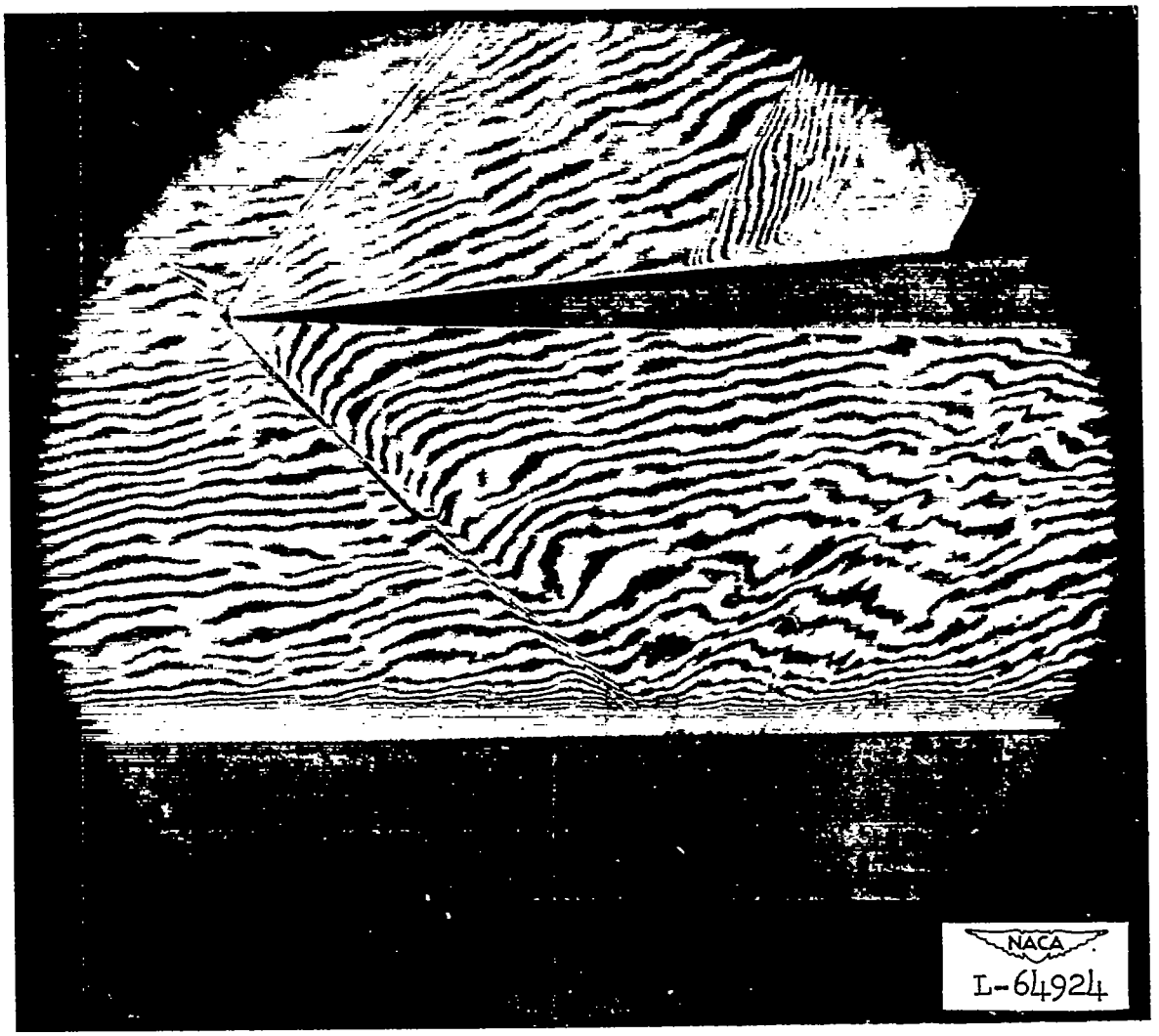

(b) $\delta = 1\frac{3^{\circ}}{4}$.

Figure 9.- Continued.

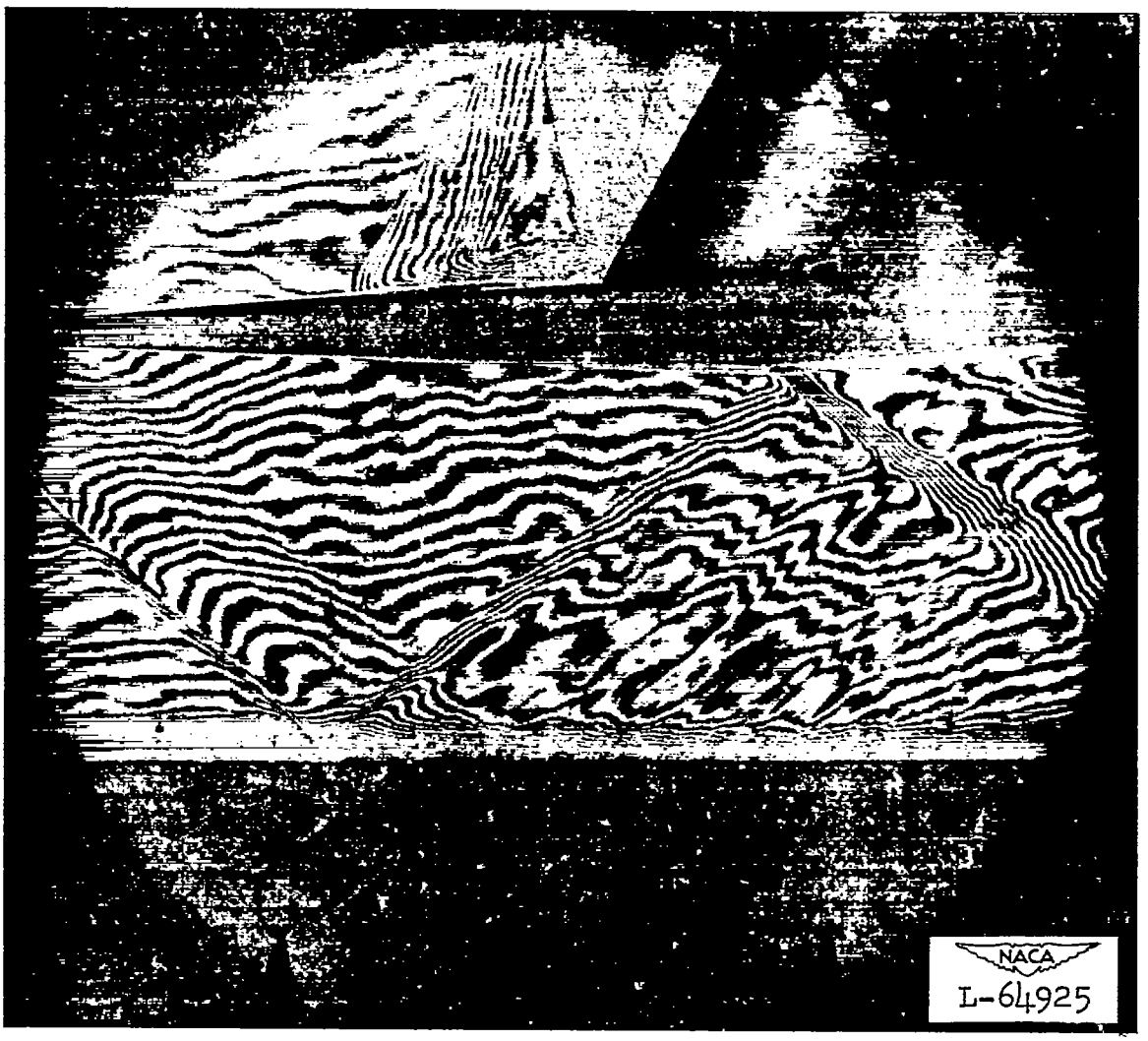

(c) $\delta = 1\frac{3}{4}^{\circ}$. Wedge moved 3/4 inch upstream.

Figure 9.- Concluded.

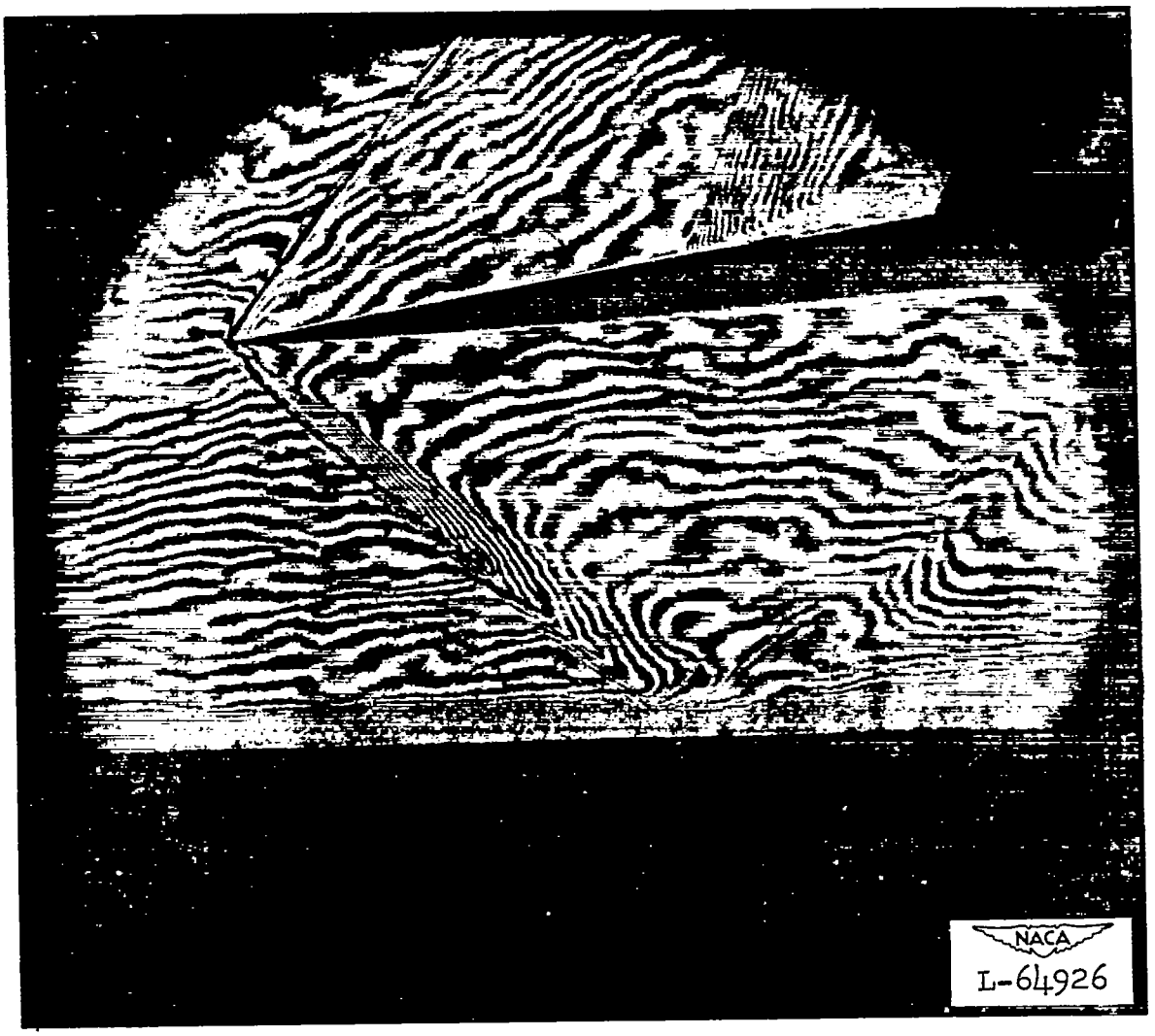

(a) $\delta = -2\frac{3}{4}^{\circ}$.

Figure 10.- Interferogram of flow in the region between a wedge and a porous wall at a Mach number of 1.62, with an expansion region originating at the leading edge of the wedge.

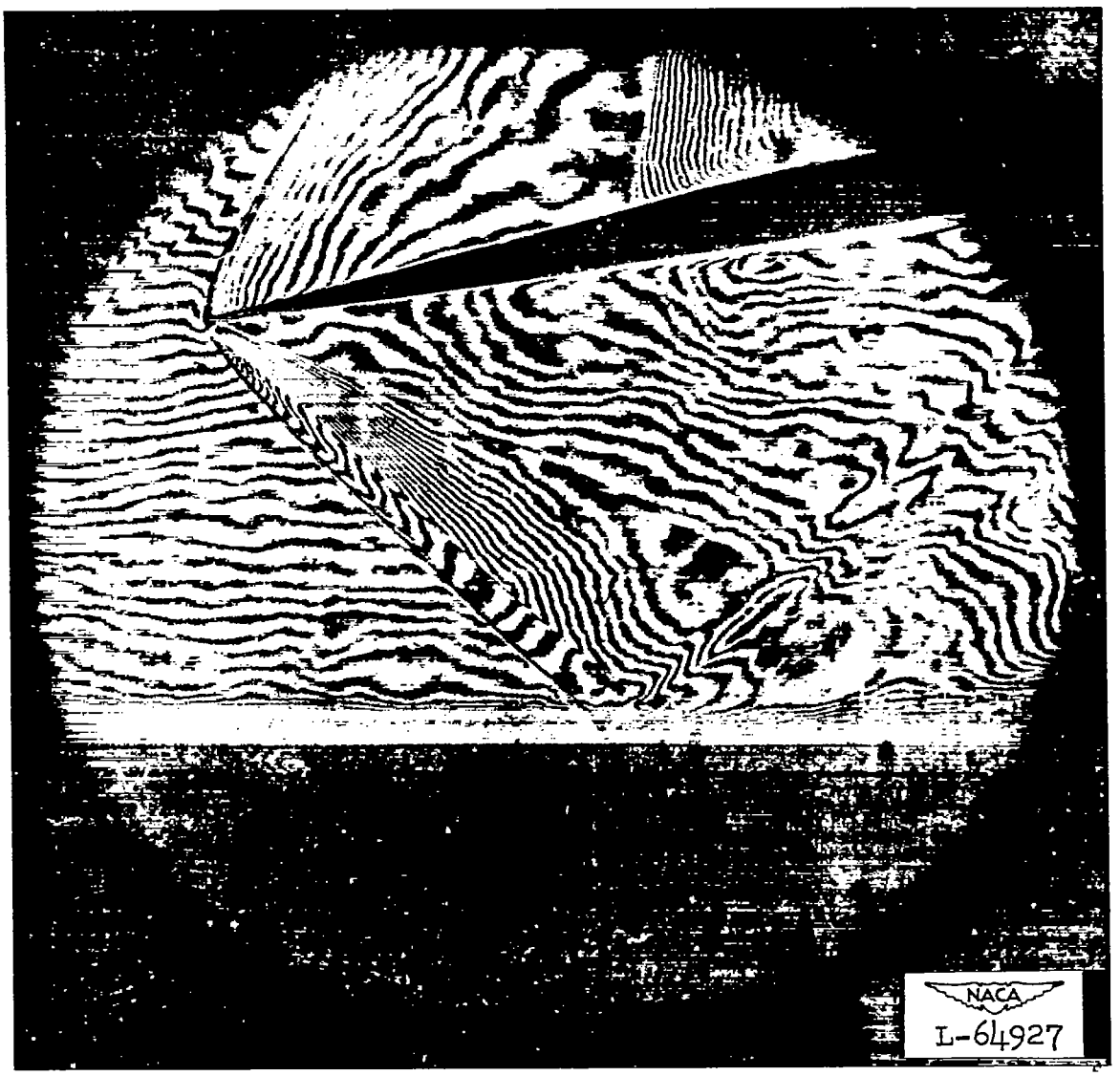

(b) $\delta = -8^{\circ}$.

Figure 10.- Concluded.